Geo-Resilience 2023 Conference, Cardiff, Wales
D.G. Toll & M.G. Winter (Eds)
British Geotechnical Association, London. 2024
https://doi.org/10.53243/Geo-Resilience-2023-6-1

An Integrated Experimental and Numerical Approach for Assessing the Hydro-mechanical Response of Flood Embankments

Elena DODARO[1], Giulia MB VIGGIANI[2], Guido GOTTARDI[1]

[1]University of Bologna, Bologna, Italy
[2]University of Cambridge, Cambridge, United Kingdom
Corresponding author: Elena Dodaro (elena.dodaro2@unibo.it)

Abstract

Extreme geohazards, such as flood events, are becoming increasingly frequent due to the major impact of climate change, with severe consequences in terms of economic damage and loss of human. Water retaining earthworks play a key role in the preservation of the built and rural environment, thus a reliable assessment of river embankment safety conditions represents an essential task to enhance the resilience of these critical infrastructures. In current engineering practice, the design and validation of flood embankments is still performed under the simplistic hypothesis of steady-state groundwater flow and generally disregarding – or possibly oversimplifying - unsaturated soil issues, mainly due to the difficulties in estimating the actual suction distribution and shear strength. In this paper, a methodological approach for accurately predicting the hydro-mechanical response of flood embankments to high water events, based on the complementary use of laboratory testing and numerical modelling, is proposed. An extensive experimental campaign, including standard and advanced suction-controlled tests, has been carried out to investigate the effect of suction changes on the shear strength and compressibility of a silty sand mixture, representative for the riverbank systems of the main river Po tributaries (Italy). Then laboratory test results have been considered to perform finite element (FE) transient seepage and stability analyses by Strength Reduction Method, finalized to the assessment of an embankment model performance, under a set of possible hydrometric peaks. Factor of safety variations over time have been estimated, in connection with the changeable water level imposed, providing some useful insights for flood risk assessment of river embankments.

Keywords: River embankments, Unsaturated soils, Transient seepage analysis, Slope stability assessment.

1. Introduction

The periodic occurrence of catastrophic flood events related to the collapse of river retaining earthworks constitutes one of the most prominent issues for hydrogeological risk management and land-use planning, usually resulting in severe damages to buildings, transport infrastructures and crops, considerable repairing costs and loss of human. Flood trends in Europe over the last few decades, have shown a rising number of devastating events, with a significant increase in annually inundated territories and a severe impact on the vulnerability of the communities living in flood-prone areas (Paprotny et al., 2018). Historical overviews worldwide reported 151 events occurring from 1960 to 1969, while between 2000 and 2009, almost 1500 floods were observed (EEA, 2018). For the EU countries, the estimated annual damage has jumped from an average of €6 billion to around €20 billion per year (Kundzewicz et al., 2013). Furthermore, the Intergovernmental Panel on Climate Change predicted that climate-related extremes will become even more frequent (IPCC, 2022). In this framework, the need for strengthening and enhancing the resilience of critical infrastructures, such as river embankments and, more generally, earthworks used for hydraulic regimentation, through a reliable stability assessment of the earth structures, together with a detailed knowledge of the pressures acting on them, represents a crucial aspect for governments and agencies in charge of flood protection and has recently received a growing attention. Nevertheless, in many European countries, minor embankments are not even subject to any formal requirements or technical guidelines. Flood embankments are still typically designed and validated under the simplified hypothesis of stationary flow regime, in equilibrium with the maximum expected river level, usually neglecting the actual pore water pressure distributions within the soil, due to a typical lack of experimental and field monitoring data. However, several research studies on full scale and small-scale riverbank physical models, as well as in-situ evidence, have proved that evapo-transpiration phenomena, water level fluctuations and suction evolution induced by the advancement of the saturation line within the embankment body during a high water event have a fundamental role in the overall earthworks performance, both in terms of infiltration regime and stability conditions (Chiang, 2011; Calabresi et al. 2013; Higo et al. 2015). In particular, pore water pressures build-up, induced by the saturation process, leading to a progressive decrease of the shear strength, has been recognized as a main triggering factor of macro-instabilities of slopes (Hooke, 1979; Thorne, 1982; Rinaldi and Casagli, 1999; Lee et al., 2017). The hydro-mechanical behaviour of flood embankments subjected to drying/wetting cycles can be properly investigated by a combination of transient seepage and stability numerical analyses, considering a suitable set of unsaturated soil geotechnical parameters. To this aim, an accurate soil characterization of a compacted silty sand mixture and of a consolidated clayey silt, representative for the filling material and the subsoil of the embankments of the river Po tributaries (Italy), has been performed under saturated and partially saturated soil conditions and is synthetically reported in this paper. The study of the transient seepage, establishing in a river embankment model, as a consequence of the water level changes, together with the estimation of the associated safety conditions of the earth structure over time, have been conducted through a fully-coupled finite element (FE) analysis and by applying the Strength Reduction Method, implemented in the PLAXIS 2D software (Plaxis, 2020).

2. Case study

A typical embankment section of the Alpine and Apennine riverbank systems of the main river Po (Northern Italy), which have recently experienced sudden overall collapses (Figure 1), has been considered for the present study. The central core of these embankments originated from alluvial sediments and, starting from the 19th century, was progressively enlarged and raised up to 5-10 meters above the ground level, using site-available natural soils, thus becoming a continuous linear infrastructure. The filling material is prevalently constituted by a heterogeneous mixture of sands and silt, while the subsoil frequently consists of clayey and silty deposits. Similarly, the soil selected for the present investigation is a compacted mixture of 70% Ticino sand (TS) and 30% Pontida clay (PON), while for the foundation, a homogeneous consolidated layer of PON is taken as reference. TS is a well-known Italian uniform coarse to medium quartz-feldspathic sand, made of angular to sub rounded particles; PON is a low plasticity kaolinitic clayey silt deriving from a quarry of fine material located in the north of Italy and deposited in a post-glacial lake environment.

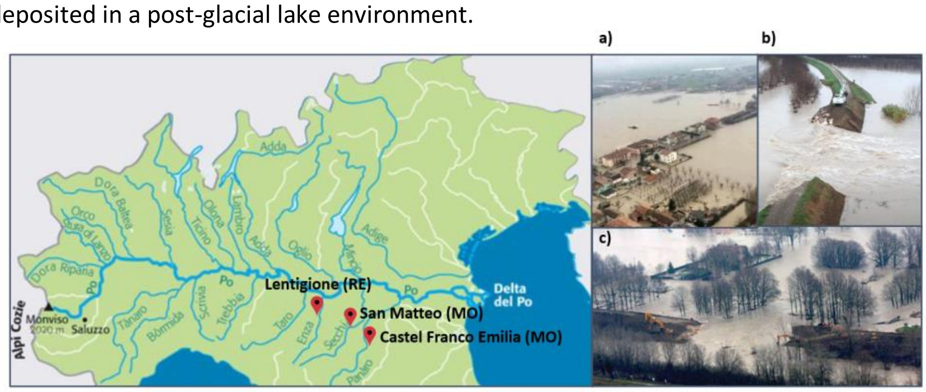

Figure 1: On the left: schematic map of the river Po catchment. On the right: recent riverbank breaches occurred in: a) Lentigione (RE), the river Enza, 2017; b) Castel Franco Emilia (MO), the river Panaro, 2020; c) San Matteo (MO), the river Secchia, 2014.

The geometry of the riverbank section analysed herein (sketched in Figure 2) has been defined as suitable for replicating a typical failure mechanism for the selected case study (i.e. the instability of the slopes) and concurrently reproducible for small-scale physical modelling. The embankment, characterized by a simple trapezoidal shape, has a height of 7.5 m above the ground level, slopes inclination of 45° and about 56° for the riverside and the landside, respectively and a 3 m-wide crest; the foundation consists of a 5 m-thick fine-grained layer.

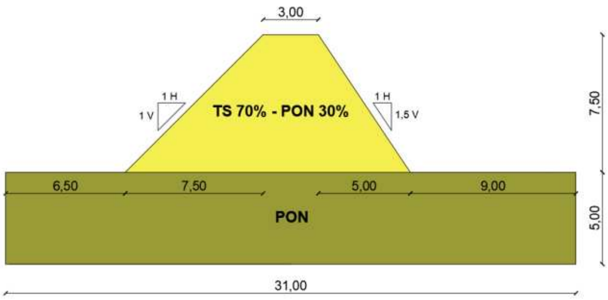

Figure 2: Geometry of the river embankment section numerically analysed.

3. Laboratory characterization of the materials

3.1 Physical properties

Particle size distributions of the TS 70% - PON 30% and its single components are plotted in Figure 3, together with a 2D projection of the mixture particles, obtained with the dynamic image analyser QICPIC, available at the National Research Facility for Infrastructure Sensing (NRFIS) of University of Cambridge (UK). Soil index and physical main properties (γ_{min} maximum value of soil unit weight, γ_{max} minimum value of soil unit weight, e_{min} minimum value of void ratio, e_{max} maximum value of void ratio, G_s specific soil density, D_{50} mean particle size, U_c uniformity coefficient, LL liquid limit, PL plastic limit, PI plasticity index) are listed in Table 1. To promote homogeneity and initial conditions consistency and, at the same time, to reproduce typical site compaction degree, all the TS 70% - PON 30% specimens were reconstituted at a target dry density and water content, using the standard Proctor compaction energy (ASTM D698-12, 2021) - w = 8.8%, γ_d = 20.6 kN/m^3, while the PON samples were preliminarily consolidated under the vertical effective stress of 200 kPa.

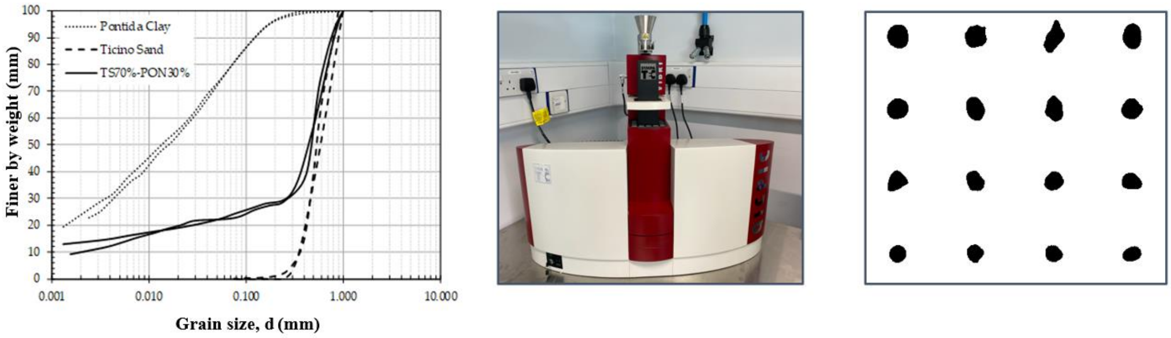

Figure 3: Particle size distribution of the investigated materials and shape of the particles of the TS 70% - PON 30% mixture. In the middle: the dynamic image analyser QICPIC (NRFIS).

Table 1: Average index and physical properties of the materials.

Soil	γ_{min}	γ_{max}	e_{min}	e_{max}	G_s	D_{50}	C_u	LL	LP	PI
	kN/m³	kN/m³	-	-	-	mm	-	%	%	%
TS	13.64	16.67	0.57	0.92	2.67	0.57	1.83	-	-	-
PON	-	-	-	-	2.74	0.02	-	23.62	13.13	10.48
TS70%-PON30%	13.48	21.31	0.24	0.95	2.68	0.46	-	17.66	10.23	7.42

3.2 Soil water retention properties

Hydraulic and retention properties of the silty sand mixture and the Pontida Clay samples have been determined from constant head permeability tests, evaporation tests and psychrometric measurements, except for the saturated permeability of the PON, which has been indirectly evaluated from two standard oedometer tests. The tensiometers-based equipment, HYPROP and the high-range psychrometer device WP4 Dewpoint potentiometer (METER Group), which measures water potentials, by determining the relative humidity of the air above a sample in a sealed chamber, have been used for estimating the Soil Water Retention Curves (SWRCs) and Hydraulic Conductivity Functions (HCFs). The non-hysteretical Mualem-van Genuchten model (1980) has been adopted for the interpretation of experimental data, through the fitting parameters: α, related to the air entry value of the soil, n, which is a function of the rate of water extraction from the soil, as soon as the air entry value has been exceeded, and l, that affects the decrease of permeability with suction.

Table 2: Hydraulic and retention parameter of the van Mualem-van Genuchten model.

Material	k_{sat}	S_{res}	S_{sat}	α	n	l
	(m/s)	(-)	(-)	(1/m)	(-)	(-)
TS70%-PON30%	$1.23\cdot10^{-7}$	0.057	1.000	0.821	1.240	-3.350
PON	$6,67\cdot10^{-10}$	0.000	1.000	0.070	1.455	0.584

3.3 Shear strength and compressibility characteristics of the materials

A series of suction-controlled consolidated drained (CD) triaxial tests has been carried out on TS 70% - PON 30% specimens with a diameter of 38 mm and a height of 76 mm, using a double-wall triaxial apparatus, available at the NRFIS. Results have been compared to the corresponding saturated tests, performed at the University of Napoli Federico II (Italy), with a Bishop & Wesley triaxial testing system, whose interpretation can be found in Ventini et al. (2021). The well-established axis translation technique (Hilf, 1956) has been used for controlling matric suction inside the samples. Total volume changes have been measured with a volume change device interposed between the inner and the outer cell. Experimental procedures were designed to highlight the effect of suction and confining stress, on the shear strength of the tested material. Variables of interest were determined under different net confining pressures ($\sigma_n - u_a$), ranging from 50 to 300 kPa and imposing typical suction values for the embankment body ($u_w - u_a$ = 0-70 kPa), assessed through field monitoring of seasonal and daily pore water pressure distribution changes. After an equalization stage, finalized to bring the soil to the suction target, the specimens were subjected to predefined confining pressures, keeping the suction value constant and then the axial load was applied at a constant rate of 0,001 mm/min. Results have been interpreted adopting the modified Mohr-Coulomb failure criterion (Fredlund et al. 2012), expressed by the following:

$$\tau = c' + (\sigma_n - u_a) \tan \varphi' + (u_a - u_w) \tan \varphi^b$$

where τ is shear strength, c' is the effective cohesion, σ_n is the normal stress, u_a the pore-air pressure, u_w the pore-water pressure, φ' is effective friction angle and φ^b is the angle describing the rate of increase in shear strength due to matric suction. The angle φ^b is approximately equal to φ' at low matric suctions and generally reduces as matric suction increases. Table 3 illustrates the shear strength parameters for the TS 70% - PON 30% obtained from each test, with the matric suction component (i.e., ($u_a - u_w$) tan φ^b) lumped with the effective cohesion, c', for the purpose of translating the three-dimensional failure envelope onto a two-dimensional representative plot. Figure 4 reports the Mohr circles of stresses and the peak and critical state lines, plotted in the q-p' space, where p'= (σ_1 - 2σ_3)/3-u_a, in the case of s = 0 kPa and s = 50 kPa. The lines obtained from suction-controlled tests exhibit an upward shift, parallel to the saturated line, which could be attributed to the apparent cohesion in the unsaturated specimens.

Table 3: Shear strength parameters of TS 70% - PON 30%, obtained at different level of matric suctions.

Matric suction, s	**Effective cohesion, c'**	**Angle of internal friction (φ')**
(kPa)	**(kPa)**	**(°)**
0	3	45.5
50	10	47.0
70	13	47.5

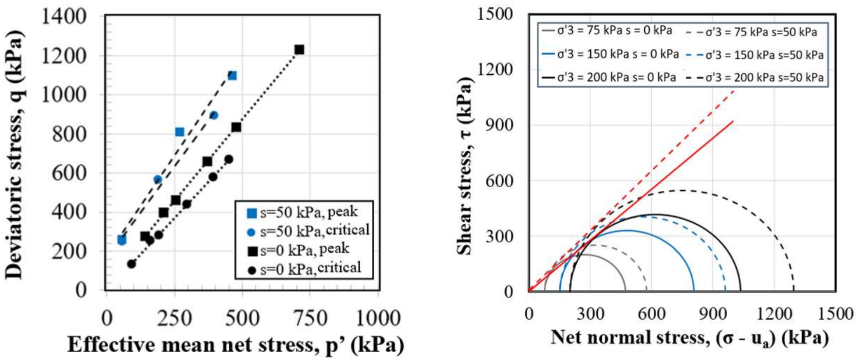

Figure 4: Peak and critical state lines on the q-p' plane and Mohr circles for saturated and unsaturated samples with s = 50 kPa.

Standard and suction-controlled oedometer tests have been carried out, using a Bishop-type oedometer apparatus and the oedometer cell manufactured by the Polytechnic University of Catalonia (UPC), to describe the evolution of the silty sand mixture compressibility, when subjected to different vertical total stress and suctions. Specimens have been reconstituted within a rigid confining ring, characterized by a diameter of 70.41 mm and a height of 20 mm. After a first equalization to a suction of 30 kPa, a drying path was imposed to the specimen, maintaining a constant mean net stress of 75 kPa (corresponding to a depth of about 6 m from the crest of the embankment), to determine the soil water retention curve of the material, under a typical confining stress for riverbank filling materials, then a standard loading-unloading pattern was imposed. From the plot of the void index-net vertical stress curves, reported in Figure 5, used for the estimation of the compressibility parameters, it can be clearly noted that the unsaturated soil specimen exhibits a higher stiffness with respect to the saturated one, both along the virgin compression path, than during the unloading stage. Soil strength and stiffness parameters of the Pontida clay have been derived through a series of standard oedometer and drained and undrained triaxial tests, carried out on both isotropically and anisotropically consolidated samples and are discussed in Ventini et al. (2021).

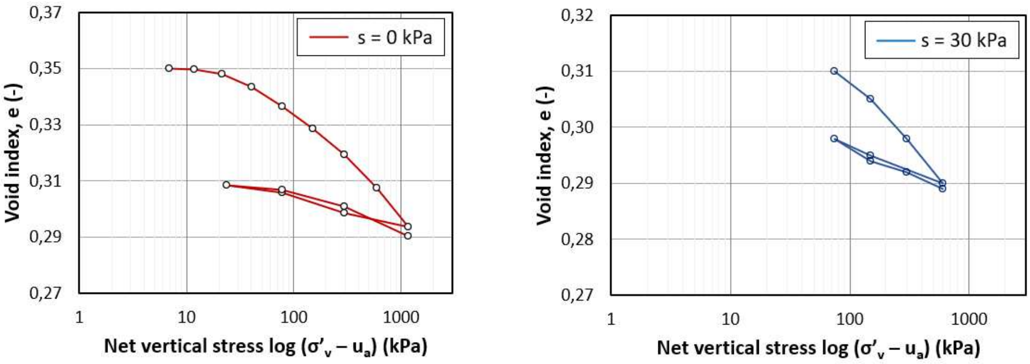

Figure 5: Oedometer loading and unloading stages for the saturated and unsaturated samples (s = 30 kPa).

4. Numerical modelling

With the aim of investigating the hydro-mechanical behaviour of the riverbank section, object of the present study towards a simulated flood event, a fully coupled transient flow-deformation analysis has been performed by means of the finite element software PLAXIS 2D. The Hardening Soil (HS) model, developed by Duncan and Chang (1970) under the framework of the plasticity theory, has been adopted for modelling the mechanical behaviour of the mixture. For the foundation layer the Modified Cam-Clay (MCC) constitutive law, an elastic-plastic strain hardening model, based on Critical State theory and proposed by Muir Wood (1990), has been considered. The model parameters assumed as input in the numerical analyses are listed in Table 4.

Table 4: Mechanical and physical parameters assigned to the embankment body and foundation units in PLAXIS 2D, according to the Hardening Soil and Modified Cam Clay (constitutive models, respectively).

	γ_{unsat}	γ_{sat}	e_{init}	E_{50}^{ref}	E_{oed}^{ref}	E_{ur}^{ref}	m	c'	f'	K_0^{NC}	ν	λ^*	κ^*	M
Material	$\frac{kN}{m^3}$	$\frac{kN}{m^3}$	-	$\frac{kN}{m^2}$	$\frac{kN}{m^2}$	$\frac{kN}{m^2}$	-	$\frac{kN}{m^2}$	°	-	-	-	-	-
TS70% - PON30%	20.8	22.3	0.30	$22.52 \cdot 10^3$	$10.00 \cdot 10^3$	$67.56 \cdot 10^3$	0.5	5.0	46.0	0.287	0.223	-	-	-
PON	17.51	21.01	0.55	-	-	-	-	-	-	0.596	0.20	0.074	0.055	1.33

4.1 Initial and boundary conditions

The definition of realistic initial conditions in terms pore water pressure distributions represents a crucial aspect for transient seepage analyses of earthen structures and the assessment of safety conditions. In the present study, a constant value of matric suction of 4,5 kPa, measured in laboratory after the preparation of the TS 70%-PON 30% specimens, has been assigned to the embankment body and the water table has been assumed in correspondence of the ground level. With the aim of investigating the hydro-mechanical behaviour of the riverbank model towards wetting and drying cycles, a time-dependent hydraulic boundary condition has been applied on the surfaces potentially affected by water action. The proposed synthetic hydrograph is characterized by three subsequent high water events, reaching the same maximum level of 6,75 m, following by drawdowns, which bring water table at progressively higher elevation; a final persistent peak has been also considered for simulating a stationary flow regime. The elapsed time of the analysis is 120 days (Figure 6).

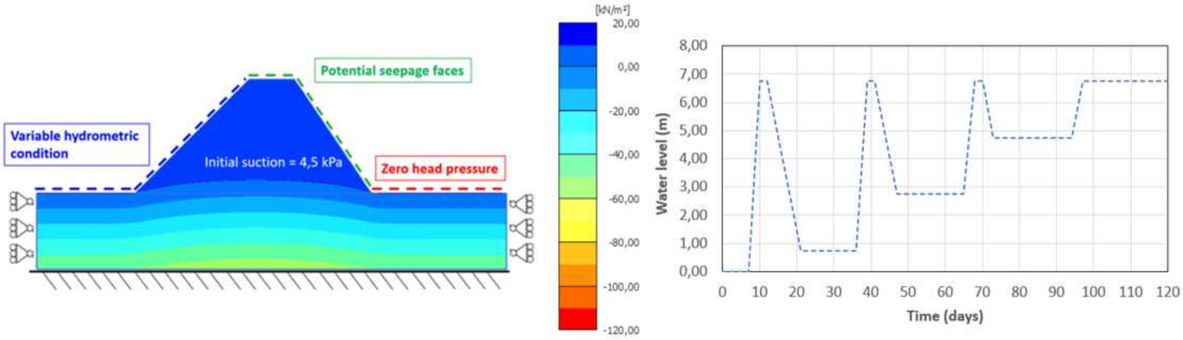

Figure 6: Initial pore water pressure distribution for transient seepage analyses (isoline increment = 10 kPa), phreatic surface in blue line and hydraulic head boundary condition assumed in the numerical study.

4.2 Results and discussion

Figure 7 summarizes the results of the transient seepage analysis in terms of pore water pressure contours, with reference to three significant time steps. Following the first water level increment, about a third of the embankment body turns out to be already in saturated conditions; this outcome can be fairly attributable to the retention properties, the significant hydraulic conductivity of the soil, as well as to the magnitude of the flood event. After the first drawdown, the phreatic surface within the riverbank does not come back to its initial configuration, on the contrary, it remains at a considerable height above the ground level. The succession of hydrometric peaks results in a gradual advancement of the phreatic surface towards the landside slope, which causes a significant increasing of the pore water pressure in the entire riverbank section and in a decrease of the suction contribution to the overall shear resistance. The incremental deviatoric strains, γ_s, which appear extremely low at the beginning of the flooding stage, tend to increase, with the advancement of the phreatic surface within the levee, highlighting the shape of a possible slip surface.

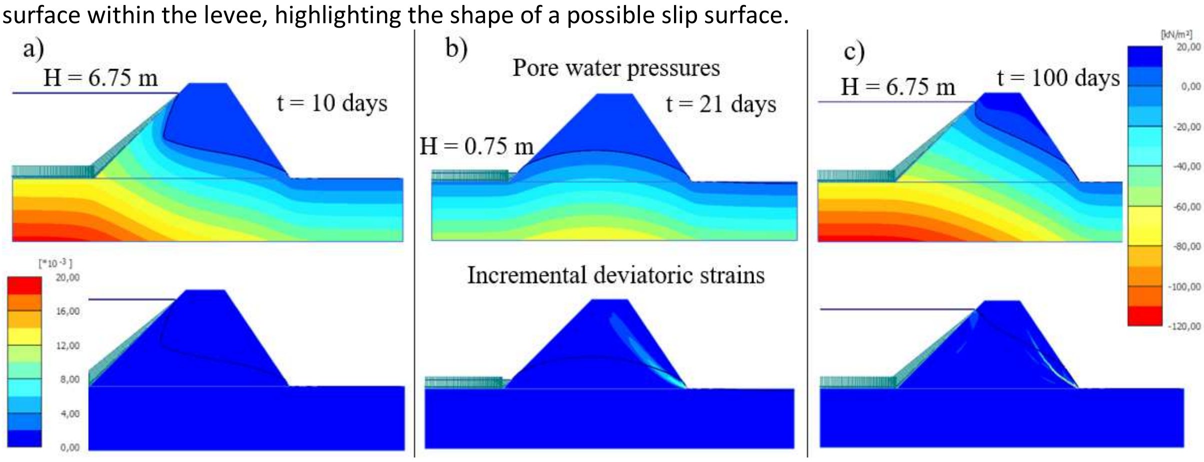

Figure 7: Pore pressures and total deviatoric strains at different stages during FEM analysis: a) after the first water level increment; b) following the first drawdown; c) during the persistence of last hydrometric peak.

The correlation between river stages and their effects in terms of stability is particularly evident observing the evolutions of the Factor of Safety (FS) over time, estimated by the Strength Reduction method, plotted in Figure 8, together with the applied hydrograph. Following the first river stage rise, a reduction in the shear strength of the riverbank material is induced by the increasing of positive pore water pressures and the consequent decrement of the suction contribution to the resistance. Hence, the FS gradually decreases during the succession of hydrometric peaks, reaching a minimum value when a stationary flow regime is attained. However, as the minimum value of the FS is greater than the unit, even after a flood event of unrealistic persistence, the embankment results to be in a stable condition for the whole elapsed period. Comparing the results in terms of factor of safety between the final step of the analysis (1.15) and that estimated in correspondence of the third hydrometric peak (1.40), it is evident that the steady-state condition is associated to a significantly lower safety margin, thus resulting in a highly conservative river embankment stability assessment.

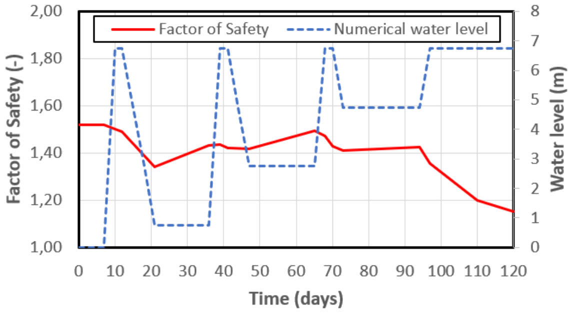

Figure 8: Variation of FS over time, compared to the numerical water level assumed.

5. Concluding remarks

A methodological approach for the investigation of the hydraulic response and stability assessment of a flood embankment model, representative for the riverbank system of the river Po tributaries (Italy), has been described in this paper. The approach is based on the combined use of standard and advanced laboratory testing and of finite element numerical modelling. Suction-controlled triaxial and oedometer tests have been performed to carefully estimate the model parameters and to highlight the significant contribution of suction to shear strength and stiffness of the silty sand mixture, composing the embankment body. A series of hydrometric peaks, followed by an unrealistically persistent high water level, able to finally establish steady-state flow conditions within the embankment, has been imposed to the riverside surfaces potentially affected by the water action, in order to study the performance of the model earth structure, under two different flow regimes. Results of numerical analyses have clearly showed that a succession of high water events may generate a progressive increase of pore pressures within the embankment body and, therefore, a significant decrease of the shear strength, potentially triggering slope failure mechanisms. In addition, the determination of safety factor variations over time has clearly demonstrated that the stationary flow regime is associated to a significantly lower safety margin, with respect to the most unfavourable scenario experienced by the earth structure, as a consequence of the water level fluctuations (corresponding to the third hydrometric peak). This means that the steady-state conditions, typically considered in the current engineering practice may lead to erroneous conclusions on the effective safety margins towards possible slope instability and result in excessively conservative stability assessment.

Acknowledgements

This research was funded under the scheme for “Research Projects of National Relevance” - PRIN 2017 Call, grant 2017YPMBWJ, promoted by the Italian Ministry of Education, University and Research (MIUR).

Eng. G. Sorrentino (Dept. of Civ. Eng., University of Cambridge, UK) is greatly acknowledged for his fundamental contribution to laboratory soil testing, while the first Author was visiting the University of Cambridge.

References

Calabresi, G., Colleselli, F., Danese, D., Giani, G., Mancuso, C., Montrasio, L. et al. (2013). Research study of the hydraulic behaviour of the Po River embankments. *Canadian Geotechnical Journal*.

Chiang, S.W., Tsai, T.L., Yang, J.C. (2011). Conjunction effect of stream water level and groundwater flow for riverbank stability analysis. *Environmental Earth Sciences*, 62, 707-715.

Duncan, J.M., Chang, C.Y. (1970). Nonlinear analysis of stress and strain in soil. Journal of the Soil Mechanics and Foundation, 96: 1629-1653.

European Environment Agency. (2018). Floods. Available online: https://www.eea.europa.eu/archived/archived-content-watertopic/ water-resources/floods

Fredlund, D. G., Rahardjo H., Fredlund M.D. (2012). *Unsaturated Soil Mechanics in Engineering Practice*. Wiley and Sons Inc., New York.

Higo, Y., Lee, C.W., Doi, T., Kinugawa, T., Kimura, M., Kimoto, S., Oka, F. (2015). Study of dynamic stability of unsaturated embankments with different water contents by centrifugal model tests, *Soils and Foundations*, 112-126.

Hilf, J. W. (1956). An Investigation of Pore Water Pressure in Compacted Cohesive Soils. Doctoral dissertation, University of Colorado, Boulder.

Hooke, J.M. (1979). An analysis of the processes of river bank erosion. *Journal of Hydrology*, 42, 39-62.

Intergovernmental Panel on Climate Change. (2022). Climate Change 2022: Impacts, adaptation and vulnerability. *Contribution of Working Group II to the Sixth Assessment Report of the Intergovernmental Panel on Climate Change*. Pörtner, H.O., Roberts, D.C., Tignor, M., Poloczanska, E.S. et al. (eds.), Cambridge University Press, UK and New York, USA.

Kundzewicz, Z.W., Kanae, S., Seneviratne, S., Handmer, J. et al. (2014). Flood risk and climate change: global and regional perspectives, *Hydrological Sciences Journal*, 59:1, 1-2. https://doi.org/10.1080/02626667.2013.857411

Lee, C.W., Kim, Y.S., Park, S.Y., Kim, D.G., Heo, G. (2017). The behavior characteristics of a reservoir levee subjected to increasing water levels. *Journal of Civil Engineering and Management*, 23, 15-27.

Muir Wood, D. (1990). *Soil Behaviour and Critical State Soil Mechanics*. Cambridge: Cambridge University Press.

Paprotny, D., Sebastian, A., Morales-Nápoles, O. et al. (2018). Trends in flood losses in Europe over the past 150 years. *Nature Communication*, 9, 1985. https://doi.org/10.1038/s41467-018-04253-1

PLAXIS 2D Connect Edition V21 (2020): Reference manual. Bentley Systems Incorporated. Delft, The Netherlands

Rinaldi, M., Casagli, N. (1999). Stability of streambanks formed in partially saturated soils and effects of negative pore water pressures: The Sieve River (Italy). *Geomorphology*, 26, 253–277.

Thorne, C. (1982). Processes and mechanisms of river bank erosion. *In Gravel-Bed Rivers: Fluvial Processes, Engineering and Management*, John Wiley & Sons Inc.: Hoboken, NJ, USA, 227-271.

Ventini, R., Dodaro, E., Gragnano, C.G., Giretti, D., Pirone, M. (2021). Experimental and numerical investigations of a river embankment model under transient seepage conditions. *Geosciences* 11, 192.